بسم الله الرحمن الرحيم

قال تعالى:

"وعلمكم ما لم تكونوا تعلمون"

صدق الله العظيم

(البقره151)

Dedication:

To my mother and father who made me the persons I am.khansaa, nadir,moca, summer baraa,ahmed,mohamed,nona,nani,Noor,jood with love

Acknowledgment:

I would like to send out my greatest thanks to:

Dr: MOHAMEDAL FADIL for kindly supervising this study and for his patience through all the month's that make this work possible.

Dr.Waddah mohamed , ahd ,reham, yousra , hiba ,sara , aza , safa ,namariq , majed , mosaab , amir, taj, habashi, rezga, bonosh ,mozafar and all my friend for endless encouragement and unlimited support.

Abstract:

This study consists of 51 patient's different age, sex whom were referred to cardiology clinic for myocardial perfusion scintigraphy. To identify the percentage of the functioning areas of the heart by computer programthe study was also designed to code the heart SPECT image according to the function,

differentiate between normal & abnormal area and

To measure the size of the heart and the defected area. The patient

underwent myocardial perfusion rest and stress scan taken after 30-40min, 50-60min respectively by acquiring 32 frames at 30sec/projectionwith the patients in supine position, in addition that in stress test the patients were injected with the pharmacological stress Persantine (0.567*patient weight) diluted with normal saline to have a total volume of 20ml. The study was conducted at International medical center (IMC) in SAUDIA ARABIA, JADDAH. Between(Oct2013-May2014). The results showed that there is a significant difference between the functioning percentage of the heart at rest and stress concerning the mild and moderate classification of heart perfusion reduction.

الخلاصة

اجريت هذه الدراسه على 51 مريض من مختلف الأعمار والأجناس (زكر او انثى) الذين ذهبوا لعيادة القلب لأجراء مسح ذري لعضلة القلب, للتعرف على النسبه المئوية لأجزاء القلب التي تعمل عن طريق الكمبيوتر,وايضا لمطابقة صورة مسح التصوير المقطعي بالفوتون الأحادي مع وظائف القلب والتمييز بين المناطق الطبيعية والتي بها خلل, ولمعرفة حجم القلب.خضع المرضى لمسح الراحةلنضحعضلة القلب و مسح الاجهد لنضح عضلة القلبالذين اتخذا بعدثلاثين الى اربعين دقيقه,اربعين الى خمسين دقيقه على التوالي من خلال الحصول على اثنين وثلاثين اطارآ باتخاذ كل اطار في ثلاثين ثانيه مع وضع المرضى في وضعية الاستلقاءوبالإضافة إلى ذلك فانه في اختبار الإجهاد قد تم حقن المرضى بدواء البيرسانتين(0.567 * وزن المريض) المولد للاجهاد المخفف بمحلول ملحي طبيعي على ان يكون الحجم الكلي للحقن عشرون مل.

أجريت هذه الدراسه في المركز الطبي الدولي جدة لمدة سبعة اشهر. واوضحت النتائج ان هنالك فرق واضح بين الفحوصات في حالة الراحة والأجهاد فيما يتعلق بالتصنيف المتقدم لأنخفاض نضخ عضلة القلب.

Table of contents:

CHAPTER TWO

CHAPTER THREE

METHODOLOGY

CHAPTER FOUR

CHAPTER FIVE:

Discussion, conclusion and recommendation

List of table

List of figures:

Chapter one
Introduction

Evaluation of suspected or known heart disease remains one of the most important application of nuclear cardiology .In the last decades, technological development have

provided many innovative diagnostic tools for the improved identification and measurement of disease, not only in nuclear medicine but also in cardiac imaging in general .Despite of all of these advances the evaluation of coronary artery disease (CAD) involves great deal of individual clinical judgment. Before proceeding with any diagnostic test, it is essential to obtain a thorough medical history and to perform a complete physical examination, formulate a diagnostic hypothesis, determine the pretest probability of disease, and define the best strategy of investigation for each patient. Nuclear cardiac studies and other complementary modalities are extremely helpful when well indicated and are invaluable diagnostic tools for evaluating the cardiac patient in current medical practice.

Although the delivery of optimal patient care is the ultimate goal, cost-efficient utilization of limited resources is a growing concern .The goal of avoiding unnecessary use of expensive invasive procedures has focused more attention on the use of noninvasive or less invasive diagnostic and therapeutic modalities, including nuclear imaging. Ultimately, it is the treating physician is responsibility to rationalize the utilization of resources for optimal patient care at reasonable cost .

1-1 Anatomy

The adult human heart has a mass of between 250 and 350 grams and is about the size of a fist. Itis situated within the chest cavity anterior to the vertebral column and posterior to the sternum. The heart divided by a partition or septum into two halves, and the halves are in turn divided into four chambers, two superior atria and two inferior ventricles. The atria are the receiving chambers and the ventricles are the discharging chambers, it is enclosed in a double-walled sac called the pericardium. It has two leaflets, the superficial is called the parietal pericardium and the inner one is the visceral pericardium. Between them there is some pericardium fluid which

function is to permit them the easy slide with the heart movements. Outside the parietal pericardium there is a fibrous layer which depends from the mediastinal fascia and is called the pericardium. This sac protects the heart, anchors it to the surrounding structures, but has no effect on ventricular hemodynamic in a health person. (Clinical anatomy by SNILL, Wikipedia.com)

The outer wall of the human heart is composed of three layers. The outer layer is called the epicedium, or visceral pericardium since it is also the inner wall of the pericardium. The middle layer is called the myocardium and is composed of cardiac muscle which contracts. The inner layer is called the endocardium and is in contact with the blood that the heart pumps. Also, it merges with the inner lining (endothelium) of blood vessels and covers heart valves.(Clinical anatomy by SNILL, Wikipedia.com)

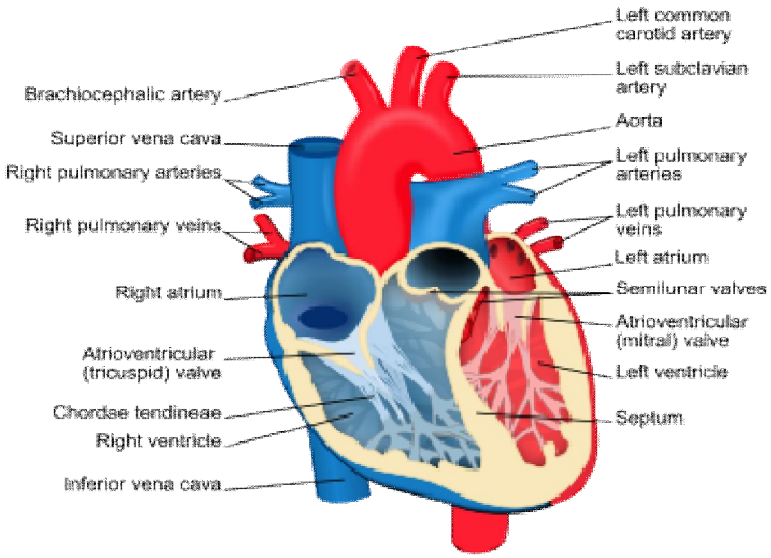

Figure 1-1 anatomical details of the heart

1-2 Physiology

In humans, the function of the right side of the heart is to collect de-oxygenated blood, in the right atrium, from the body (via superior and inferior vena cava) and pump it, through the tricuspid valve, via the right ventricle, into the lungs (pulmonary circulation) so that carbon dioxide can be dropped off and oxygen picked up (gas exchange). This happens through the passive process of diffusion. The left side collects oxygenated blood from the lungs into the left atrium. From the left atrium the blood moves to the left ventricle, through the bicuspid valve (mitral valve), which pumps it out to the body (via the aorta). On both sides, the lower ventricles are thicker and stronger than the upper atria. The muscle wall surrounding the left ventricle is thicker than the wall surrounding the right ventricle due to the higher force needed to pump the blood through the systemic circulation.

The aorta forks the blood and it is thendivided between major arteries which supply the upper and lower body. The blood travels in the arteries to the smaller arterioles and then, finally, to the tiny capillaries which feed each cell. The (relatively) deoxygenated blood then travels to the venules, which coalesce into veins, then to the inferior and superior venacava and finally back to the right atrium where the process began.(Anatomy & physiology for ROSS &WILSON, wikipedia.com)

The heart is effectively a syncytium, a meshwork of cardiac muscle cells interconnected by contiguous cytoplasm bridges. This relates to electrical stimulation of one cell spreading to neighboring cells.(Anatomy & physiology for ROSS &WILSON, wikipedia.com).

Some cardiac cells are self-excitable, contracting without any signal from the nervous system, even if removed from the heart and placed in culture. Each of these cells have their own intrinsic contraction rhythm. A region of the human heart called the sinoatrial (SA) node, or pacemaker, sets the rate and timing at which all cardiac muscle cells contract. The SA node generates electrical impulses, much like those produced by nerve cells. Because cardiac muscle cells are electrically coupled by inter-calated disks between adjacent cells, impulses from the SA node spread rapidly through the walls of the atria, causing both atria to contract in unison. The impulses also pass to another region of specialized cardiac muscle tissue, a relay point called the atrioventricular node, located in the wall between the right atrium and the right ventricle. Here, the impulses are delayed for about 0.1s before spreading to the walls of the ventricle. The delay ensures that the atria empty completely before the ventricles contract. Specialized muscle fibers called Purkinje fibers then conduct the signals to the apex of the heart along and throughout the ventricular walls. The Purkinje fibers from conducting pathways called bundle branches. This entire cycle, a single heartbeat, lasts about 0.8 seconds. The impulses generated during the heart cycle produce electrical currents, which are conducted through body fluids to the skin, where they can be detected by electrodes and recorded as an electrocardiogram (ECG or EKG). The events related to the flow or blood pressure that occurs from the beginning of one heartbeat to the beginning of the next can be referred to a cardiac cycle.(Anatomy & physiology for ROSS &WILSON, wikipedia.com).

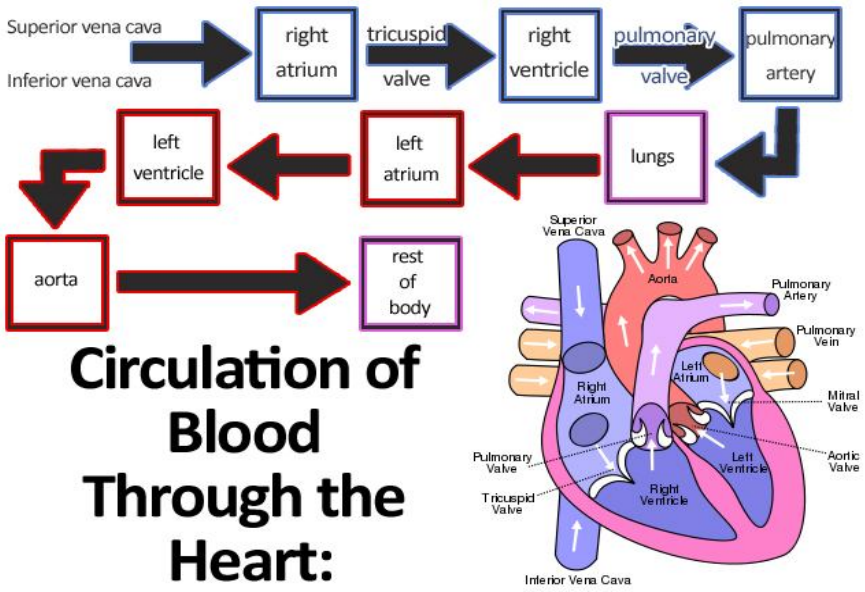

Figure 2

1-3 Pathology

Cardiovascular disease (heart disease) refers to any disease that affects the cardiovascular system, principally cardiac disease, vascular diseases of the brain and kidney, and peripheral arterial disease. The causes of cardiovascular disease are diverse but atherosclerosis and/or hypertension are the most common. Additionally, with aging come a number of physiological and morphological changes that alter cardiovascular function and lead to subsequently increased risk of cardiovascular disease, even in healthy asymptomatic individuals.

Cardiovascular disease is the leading causes of deaths worldwide, although cardiovascular disease usually affects older adults, the antecedents of cardiovascular disease, notably atherosclerosis, begin in early life, making primary prevention efforts

necessary from childhood.Atherosclerosis and Impaired coronary blood flow reserve (CBFR) –The basis of nuclear cardiology. Human atherosclerosis is a dynamic process that begins early and progresses through life. Risk factors, smoking, hypertension (HTN), hypercholesterolemia, diabetes mellitus (DM) or a positive family history of coronary artery disease (CAD) are well known to accelerate the atherosclerotic process,which naturally affect all human being. Atherosclerotic lesions may or may not affect myocardial blood flow (MBF) to a certain region of the heart, depending basically on the degree of impairment of the dilatory capacity of the coronary arteries and,importantly, the quantity and quality of collateral vessels. In term of myocardial area at risk,these two factors are more important than the degree of vessel obstruction alone .In this context a moderately obstructive lesion of 50 %, involving importantly the vessel wall, to the point of impairing its ability to dilate in response to exercise, may cause more myocardial ischemia than a 90% obstruction with a rich collateral circulation.

With progression, atherosclerotic lesions may impair coronary blood flow reserve (CBFR), initially affecting MBF during stress/exercise and at a later stage at rest. The stress tests most commonly used for evaluation of CBFR include the treadmill test (TMT) alone and rest/stress myocardial perfusion scintigraphy (MPS) using various methods for stress testing, including exercise, dipyridamole, adenosine, or dobutamine. Alternative protocols include low-level physical exercise combined with dipyridamole or adenosine.

1-4 Myocardial perfusion imaging

In cardiology, nuclear medicine imaging has assumed an important role in the diagnosis as well as the management of patients with coronary artery disease.

Myocardial perfusion imaging is the most widely used approach in patients with suspected cardiac disease. Perfusion imaging of the heart is highly accurate for detecting the presence of coronary artery disease. In addition, the test can predict a patient's risk for further cardiac disease (e.g., non-fatal heart attack) and cardiac death. This allows physicians to provide better care to patients with advanced and disabling. Cardiac disease by guiding therapeutic decisions; the therapies can range from conservative, drug-based management of disease to more aggressive forms of intervention, such as surgery to restore blood flow. Because of the high prevalence of coronary artery disease, myocardial perfusion imaging studies have become the most widely used nuclear medicine imaging test.

1-5 Radiopharmaceuticals

Radiopharmaceutical is defined as a radioactive compound with a property of targeting to non tar-geting ratio, when administered for purposes of diagnosis or therapy, elicits no physiological re-sponse or an adverse reaction from the patient. Any radiopharmaceutical has both chemical and physical properties which determine its physiological and imaging characteristics respectively. Practical consideration such as ease of preparation and cost are also important. Three radiopharmaceuticals are use in routine clinical use in myocardial perfusion scintigraphy:

1-5-1 ^{201}TI as a Perfusion agent

^{201} TI. Is an analog of potassium , after the initial experiences using potassium-43 , which enters viable myocardial cells by passive diffusion and also by an active mechanism involving the sodium-potassium adenosine triphosphatase pump . Only 4%to 5% of the injected dose of 2.0to 3.5 mci concentrates in the myocardium , the remainder being distributed to skeletal muscle and other tissues .The physical half-life

of thallium201 ^{201}(TI) is approximately 72 hour , but it is half-life in the myocardium is significantly shorter . During its decay,^{201}TI emits low-energy x-ray of approximately 70 kev .^{201}TI is usually administered at peak stress and distributes in the myocardium proportionally to blood flow at stress.One of the most clinically important characteristics of ^{201}TI is its redistribution over time. Redistribution is a phenomenon by which an agent dynamically cross the cell membrane, recirculates into the coronary vessels, and becomes concentrated in the myocardium proportionally to resting blood flow, this property form the basis of stress-redistribution imaging protocols used to diagnose CAD with ^{201}TI . With ^{201}TI redistribution is significant, and acquisition of stress images should being soon after the isotope is injected, preferably within 10 to 20 minutes. The longer the redistribution time, the more likely it is that ^{201}TI will redistribute within viable cells with an intact cell membrane – cells that were ischemic and had decreased uptake during stress. Therefore ^{201}TI is often used to differentiate viable tissue from scar tissue. In this regard, ^{201}TI has advantage over agent labeled with technetium 99 m (^{99m}Tc), which do not redistribute significantly.

1-5-2 ^{99m}Tc-Labled agent

Cellular uptake of cationic perforation agents, such as ^{99m}Tc-sestamibi and tetrofosmin , is mediated by a nonspecific charge-dependent transfer of lipophilic cations across the sarcolemma but is independent of Na^+ /K^+ channels . Therefore cellular uptake is not affected by cation channel inhibitor. Intracellularly , ^{99m}Tc-sestamibi appears to bind to the mitochondria in myocardial cells . Damaged nonviable cells do not maintain membrane potential, so ^{99m}Tc-sestamibi does not accumulate within nonviable cells.

Advantage of ^{99m}Tc-sestamibi

-Rapid clear from the blood pool with a peak activity at 1 minute post injection.

-Has a slow clearance rate from the heart. Its effective half- life is 3 hour.

-Is its underestimation of the extent of viable myocardium in comparison with ^{201}TI studies using a reinjection or 24 –hour redistribution protocol.

^{99m}Tc-tetrofosmin :-

Is used in similar way to ^{99m}Tc-sestamibi;blood clearance and hepatic excretion are rapid compared with ^{99m}Tc-sestamibi. Therefore ^{99m}Tc-tetrofosmin causes less hepatic artifact ,but the myocardial uptake plateaus at a slightly lower flow rate than ^{99m}Tc-sestamibi . Overall , in clinical practice these two tracer are felt to be equivalent .

The isotope ^{99m}Tc

Is widely used in nuclear medicine because :Energy 140 kev, inexpensive and ready available, Short half-life (6 hour), ^{99m}Tc permits it to be given in higher dosage than ^{201}TI ,resulting in higher count statistics with resultant better image resolution and quality, the higher count rate allows high-quality gated image to be acquired in order to assess wall motion and ventricular function simultaneously with perfusion, owing to the absence of significant redistribution , both supine and prone (or right lateral) imaging.

The energy emitted by the various isotopes may affect the choice of agent. For example, in patient with a large body it may be wise to use a higher-energy tracer, such as ^{99m}Tc-sestamibi because there is less soft tissue attenuation than with lower-energy-emitting tracer such as ^{201}TI.

The disadvantage of ^{99m}Tc-sestamibi and ^{99m}Tc-tetrofosmin compared to ^{201}TI are reduced linearity with flow, increased hepatic and splanchnic uptake, and less common lung uptake as an indicator of LV dysfunction.

1-6Problem of the study

The heart is a vital organ which is responsible for pumping blood to all other body organs. As a result of its importunateness, its diseases are critical and that is why its diagnoses must be taken seriously and the results must be 100% reliable. As a result of all of the above ,doing quantitative analysis by computer program to identify the abnormal part of the heart and normal one .

1-7 Objectives

The general objective of this study was to identify the percentage of the functioningareas of the heart in order to obtain quantitative objective evaluation of the hear condition

Specific objectives

- To code the heart SPECT image according to the function
- To differentiate between normal & abnormal area.
- To measure the size of the heart and the defected area
- To calculate the percentage of working aspect

1-8 Significance of the study

This study will provide an objective method to differentiate between normal and abnormal part of the heart as well as it will identify the percentage of normality provide specific diagnoses

1-9 Overview of the study

This study consisted of five chapters; with Chapter one is an introduction which includes: anatomy, physiology, general pathology of the heart, problem of the study, objectives, significant of the study and the overview,then Chapter two which is a

literature review that includes a comprehensive review of the scholarly literature. The material and method were cited in Chapter three. Chapter four includes result presentation and finally Chapter five includes; dissection, conclusion, and recommendations.

Chapter two
Literature review

Wong et al. (2012) studied acute myocardial infarction using Clinical features and outcomes in young adults in Singapore; in order to investigate the clinical features and in-hospital outcomes of young adults with acute myocardial infarction (AMI) in Singapore. Their study consisted of 333 patients. Their inclusion criteria include: the

presence of chest pain and/or electrocardiographic changes suggestive of infarction or ischaemia, associated with increased level of cardiac troponins or cardiac enzymes to at least twice the upper limit of the normal value. All the study patients underwent coronary angiography during the index hospitalisation. Angiographic stenosis was defined as diameter reduction of $\geq$ 50%. The culprit artery for AMI was identified based on morphology including complete occlusion, thrombus and ulcerative stenosis or assumed to be the tightest stenosis if these features were absent. The classification of body weight by body mass index (BMI) was according to the World Health Organization recommendation for an Asian population. A BMI of more than 27 kg/m^2 was defined as obese. The major clinical outcomes (in-hospital) analysed in our study include all-cause mortality, congestive heart failure (New York Heart Association class iii-iv), major arrhythmia events (complete heart block, ventricular tachycardia/fibrillation) and cardiogenic shock. Their results showed that, the most common risk factor was smoking (74%) followed by antecedent hypertension (28.5%), hyperlipidemia (20%) and diabetes mellitus (16.5%). The mean BMI was 26.1 ± 3.8 kg/m^2 with 37% of young adults considered obese by Asian BMI criteria. The most common risk factor newly identified at presentation was hyperlipidemia (28%) followed by diabetes mellitus (13%) and hypertension (3%).

Vijayvergiya et al. (2012) studied Post-myocardial infarction giant left ventricular pseudoaneurysm presenting with severe heart failure ;In order to discussed the role of various imaging modalities and the surgical treatment of pseudoaneurysm; in a case report study. Their study consisted of A 42-year-old male had an acute anterior wall MI. during surgery they found densely adherent to the pericardium and adjacent lingular segment of the left lung. Under cardioplegic arrest, the pseudoaneurysm was opened, leaving a small rim of sac wall towards the lung. The pseudoaneurysm had a

circular gap of about 30 mm diameter through which it was connected to the LV cavity . Their results showed that, the clinical presentation may vary depending upon congestive heart failure, mitral regurgitation, ventricular tachy-arrhythmia, systemic thrombo-embolism and cardiac rupture. In general, patients do not have specific symptoms pertaining to pseudoaneurysm, hence the diagnosis may be delayed.

Meade et al. (1978) developed Quantitative Methods in the Evaluation ofThallium-201 Myocardial Perfusion Images; in order to develop quantitative methods to assist the observer in the evaluation of thallium-201 myocardial perfusion images. Thirty-four patients, referred to the cardiac catheterization laboratory for evaluation of chest pain, were studied. Each was given a detailed clinical examination, chest x-ray, and standard 12-lead elctrocardiogram. Left ventriculograms and selective coronary cineangiograms were obtained from all patients. Fifty percent or more narrowing of the coronary arterial lumen was considered significant. The diagnosis of previous myocardial infarction was based on history, standard electrocardiogram, and the presence of akinetic or dyskinetic segments as observed in the left ventriculogram. Their result showed that the graphical presentation showing relative radionuclide activity as a function of location in the myocardium uses data obtained from the enhanced image. Out of 17 patient suffering from myocardial infarction diagnosed by angiography, 13 showed infarction by computerized thallium imaging. Ten patients showed transient ischemia by angiography and nine by imaging. There were seven normal angiograms and six normal images. There was greater than 75% correspondence in all categories.

Hachamovitch et al. (1995) made Exercise Myocardial Perfusion SPECT in Patients Without Known Coronary Artery Disease Incremental Prognostic Value and Use Risk

Stratification; in order to evaluated the incremental prognostic value, the role in risk stratification, and the impact on patient management of myocardial perfusion single-photon emission computed tomography (SPECT) in a population of patients without prior myocardial infarction, catheterization, or revascularization. They were examined 2200 consecutive patients who at the time of their dual-isotope SPECT had not undergone catheterization, coronary artery bypass surgery, or percutaneous transluminal coronary angioplasty and had no known history of previous myocardial infarction. Their result showed nuclear testing added incremental prognostic value after inclusion of the most predictive clinical and exercise variables (global $\chi 2=12$ for clinical variables; 31 for clinical exercise variables; 169 for nuclear variables; gain in $\chi 2$, $P<.0001$ for all; receiver-operating characteristic areas: 0.66±0.04 for clinical, 0.73±0.04 for clinical+ exercise variables, 0.87±0.03 for nuclear variables, p =.03 for gain in area with exercise variables; $P<.001$ for increase with nuclear variables).

Gibson et al. (1983) assessed regional myocardial perfusion before and after coronary revascularization surgery by Quantitative Thallium-201 scintigraphy. Because thallium-201 uptake relates directly to the amount of viable myocardium and nutrient blood flow, the potential for exercise scintigraphy to predict response to coronary revascularization surgery . Their study consisted of 47 patient s who had primary isolated coronary artery bypass graft surgery at the University of Virgirua Medical Center. Each patient underwent diagnostic cardiac catheterization and symptom-limited exercise thallium-20 I scintigraphy before and after surgery. Postoperative studies were obtained without respect to symptoms; after obtaining informed written consent. Their result was Forty-two patients (89%) were asymptomatic at the time of their postoperative evaluation. Four of the remaining five patients noted significant but incomplete anginal relief, and one patient with atypical angina before surgery

claimed no change after surgery. Postoperatively, the mean functional class of the patients was significantly improved to 1.1± 0.3 compared with the preoperative functional class (2.7± 0.9, p <0.001).

Nishina et al.(2006) Combined Supine and Prone Quantitative Myocardial Perfusion SPECT by using Method Development and Clinical Validation in Patients with No Known Coronary Artery Disease; in order to diagnostic value of prone imaging alone or combined acquisition using quantitative analysis. A total of 649 patients referred for MPS comprised the study population. Separate supine and prone normal limits were derived from 40 males and 40 females with a low likelihood (LLK) of CAD using a 3 average-deviation cutoff for all pixels on the polar map. These limits were applied to the test population of 369 consecutive patients (65% males; age, 65±13 y; 49% exercise stress) without known CAD who had diagnostic coronary angiography within 3 MO of MPS. Total perfusion deficit (TPD), defined as a product of defect extent and severity scores, was obtained for supine (S-TPD), prone (P-TPD), and combined supine–prone datasets (C-TPD). The angiographic group was randomly divided into 2 groups for deriving and validating optimal diagnostic cutoffs. Their result was C-TPD had a larger area under the receiver-operating-characteristic (ROC) curve than S-TPD or P-TPD for identification of stenosis ≥70% (0.86, 0.88, and 0.90 for S-TPD, P-TPD, and C-TPD, respectively; $P < 0.05$). In the validation group, sensitivity for P-TPD was lower than for S- or C-TPD ($P < 0.05$). C-TPD yielded higher specificity than S-TPD and a trend toward higher specificity than P-TPD (65%, 83%, and 86% for S-, P-, and C-TPD, respectively, $P < 0.001$; vs. S-TPD and $P = 0.06$ vs. P-TPD). Normalcy rates for C-TPD were higher than for S-TPD in obese LLK patients (78% vs. 95%, $P = 0.001$).There for Combined supine–prone quantification

significantly improves the area under the ROC curve and specificity of MPS in the identification of obstructive CAD compared with quantification of supine MPS alone.

Germano et al. (1995) developed automatic quantification of ejection fraction from Gated Myocardial Perfusion SPECT; They have developed a completely automatic algorithm in order to quantitatively measure left ventricular ejection fraction(LVEF)from gated ^{99m}Tc-sestamibi myocardial perfusion SPECT images. The algorithm for measuring LVEF was tested in 65 clinical patients undergoing 16-interval and 8-interval rest-gated SPECT and validated against first-pass radionuclide ventnculography. Their result was automatic segmentation and contouring of the LV was successful in 65/65 (100%) of the studies. Agreement between EFs measured from 8-interval gated SPECT and EFs calculated from first-pass data was high ($y = 2.44 + 1.03x$, $r = 0.909$, $p < 0.001$, s.e.e. = 6.87).Agreement between EF values measured from 16-interval and 8-interval gated SPECT was excellent($y = -2.7+ 0.97x$, $r = 0.988$, $p < 0.001$, s.e.e. = 2.65), the latter being on average lower by 3.71percentage points. Thus automatic method is rapid and highly agrees with conventional radionuclide measurements of EF thus providing clinically useful additional information to complement myocardial perfusion studies.

Germano et al. (1997) developed automatic quantitation of Regional Myocardial Wall Motion and thickening from gated technetium-99m Sestamibi Myocardial Perfusion Single-Photon Emission Computed Tomography; for the measurement of regional myocardial wall motion and wall thickening from three-dimensional gated technetium-99m sestamibi myocardial perfusion single-photon emission computed tomographic images. The algorithm was tested using a “variable thickness” heart phantom, and the quantitative results were compared with visual segmental

assessment of myocardial motion and thickening in 79 clinical patients with a wide range of ejection fractions (6% to 87%). Their result showed that significant inverse linear relations exist between the global (summed) visual motion score and the average quantitative motion, and between the global (summed) visual thickening score and the average quantitative thickening. Automatic quantitative ejection fraction measurements correlated extremely well with average quantitative motion (r = 0.929) and thickening (r = 0.959).Conclusions. There for algorithm is accurate and may be the first automatic technique for the quantitative three-dimensional assessment of regional ventricular function in cardiology.

Germano et al. (1994) did a quantitative phantom analysis of artifacts due to hepatic activity in technetium-99m myocardial perfusion SPECT studies; They observed that filtered back projection may cause arti-factual decreased myocardial wall uptake in the reconstructed images it the hepatic-to-cardiac activity ratio (HCR) in ^{99m}Tc. Clinical myocardial SPECT studies is sufficiently high (>1). They modified a commercial chest and heart phantom was modified with the addition of a customized liver insert, which was filled with various concentrations of ^{99m}Tc to simulate HCRs of O:1, I :1and 2:1 . The phantom was imaged with a high-sensitivity, three detector camera, low-energy, high-resolution (LEHR) collimation and 180° noncircular orbits. Their result was quantitative circumferential profile analysis of the reoriented SPECT images demonstrated artifactual inferior/inferoseptal maximal activity decreases of 17.8% and 462% for the 1:1 and 2:1 HCRs, compared to the 0:1 HCR. Hepatic scatter probably partly multi gates the decrease. Smoothing the projection data before reconstruction worsened the artifacts' severity. Using Butterworth filters of order 5 and cutoff frequencies of 0.1, 0.2 and 0.215 Nyquist (clinical standard) resulted in

artifactual inferior wall activity decreases of 5%, 8% and 16%, compared to using the same filter with a cut off of 0.3 for an HCR of 2:1. There for the occurrence and severity of artifactual perfusion defects is directly proportional to the ratio of hepatic-to-cardiac activity for a given level of smoothing, and linearly proportional to the amount of smoothing for a given hepatic-to-cardiac activity ratio.

Matsumoto et al. (2001) assessed quantitative assessment of motion artifacts and validation of a new motion-correction program for myocardial perfusion SPECT ; In order to studied the pattern and extent of defects induced by simulated motion and validated a new automatic motion-correction program for myocardial perfusion SPECT. Vertical motion was simulated by upward shifting of the raw projection datasets in a returning pattern (bounce) and in a nonreturning pattern at 3different phases of the SPECT acquisition (early, middle, and late), whereas upward creep was simulated by uniform shifting throughout the acquisition. Lateral motion was similarly simulated by left shifting of the raw projection datasets in a returning pattern and in a nonreturning pattern. Simulations were performed using single- and double-head detectors, and simulated motion was applied to projection images from 8 patients who had normal 99mTc-sestamibi SPECT findings. Additionally, images from 130 patients with actual clinical motion were assessed before and after motion correction. Their result was12 bounce simulations, the bouncing motion failed to produce significant (.3%) perfusion defects with either the single- or the double-head detector. With the single-head detector, early shifting created the largest defect, whereas with the double head detector, shifting during the middle of the acquisition created the largest defect. With regard to upward creep, defects were of larger extent with the double- than the single-head detector. With the single-head detector, 8 of 20 simulated motion patterns yielded significant perfusion defects of the left ventricle, 7

(88%) of which were significantly improved after motion correction. With the double-head detector, 12 of 20 patterns yielded significant defects, all of which improved significantly after correction. Of 2,600 segments in the 130 patients with actual clinical motion, only 1.3% (30/2,259) of segments that were considered normal (score = 0 or 1) changed to abnormal (score = 2–4) after motion correction, whereas 27% (92/341) of abnormal segments were reclassified as normal after motion correction. There for artifactual perfusion defects created by simulated motion are a function of the time, degree, and type of motion and the number of camera detectors. Application of an automatic motion-correction algorithm effectively decreases motion artifacts on myocardial perfusion SPECT images.

Sharir et al. (2001) studied quantitative analysis of regional motion and thickening by gated myocardial perfusion SPECT: normal heterogeneity and criteria for abnormality; In order to assess normal heterogeneity and developed and validated normal limits for quantitative regional motion and thickening by gated myocardial perfusion SPECT. Patients underwent rest 201Tl/exercise^{99m}Tc-sestamibi gated SPECT. Reference values of motion and thickening for 20 myocardial segments were obtained in 105 patients with, 5% likelihood of coronary disease (lowlikelihood group). Criteria for abnormality of motion and thickening were defined for each segment, using receiver operator characteristic analysis, in 101 patients with coronary disease (training group).. Their result showed Normal thickening decreased substantially along the longitudinal axis of the left ventricle, from 69% ± 13% at the apex to 25% ± 11% at the basal segments, whereas normal motion varied within the same ventricular plane. Validation of the criteria for abnormality yielded high accuracy in the detection of motion abnormalities (sensitivity, 88%; specificity, 92%)

and thickening abnormalities (sensitivity, 87%; specificity, 89%). Quantitative motion and thickening segmental scores showed good agreement with visual scores. The assignment of segment-specific threshold values for defining motion and thickening abnormalities provided reasonably accurate identification and grading of regional myocardial dysfunction. There were others studies using different instrumentation such as:

Motwani1et al (2014) did quantitative three-dimensional cardiovascular magnetic resonance myocardial perfusion imaging in systole and diastole; In order to addresses limitation of Two-dimensional (2D) perfusion cardiovascular magnetic resonance (CMR). Study consist of thirty-five patients underwent 3D-perfusion CMR with data acquired at both end-systole and mid-diastole. MBF and myocardial perfusion reserve (MPR) were estimated on a per patient and per territory basis by Fermi-constrained deconvolution. Significant CAD was defined as stenosis ≥70% on quantitative coronary angiography. Their result was twenty patients had significant CAD (involving 38 out of 105 territories). Stress MBF and MPR had a high diagnostic accuracy for the detection of CAD in both systole (area under curve [AUC]: 0.95 and 0.92, respectively) and diastole (AUC: 0.95 and 0.94). There were no significant differences in the AUCs between systole and diastole p values >0.05). At stress, diastolic MBF estimates were significantly greater than systolic estimates (no CAD: 3.21 ± 0.50 vs. 2.75 ± 0.42 ml/g/min, $p < 0.0001$; CAD: 2.13 ± 0.45 vs. 1.98 ± 0.41 ml/g/min, $p < 0.0001$); but at rest, there were no significant differences (p values >0.05). Image quality was higher in systole than diastole (median score 3 vs. 2,p = 0.002).

Gulati et al (2005) studied Non-invasive diagnosis of coronary artery disease with 16-slice computed tomography; the gold standard for the diagnosis of coronary artery

disease (CAD) is catheter angiography. However, catheter angiography is invasive and may not always be followed by interventional therapy. The study consist of thirty-one patients (26 with chronic stable angina, 5 with coronary anomalies) underwent 16-slice MSCT and catheter angiography. Vessels <1.5 mm in diameter were excluded. They found that The sensitivity, specificity, positive and negative predictive values of MSCT were 85% (95% confidence interval [CI]: 73–93), 94% (95% CI:90-96), 76% (95% CI: 64–85) and 96% (95% CI: 93–98), respectively. MSCT correctly classified patients with no, single-, double- and triple-vessel disease in 87% of cases. One patient was incorrectly excluded on MSCT; catheter angiography showed 50%–70% stenosis in this case. Patients with obstructive CAD had a higher Agatston score equivalent (p=0.03).There was no significant effect of heart rate on distal segment visibility. MSCT correctly identified all coronary anomalies.

Gunnarsson et al. (2001) studied ECG criteria in diagnosis of acute myocardial infarction in the presence of left bundle branch block; In order to evaluate the criteria suggested by Sgar-bossa et al. as well as studied if they might bear prognostic information. Study consists of One hundred fifty eight patients with left bundle branch block and suspicion of acute myocardial infarction, admitted to 14 Swedish coronary care units. Their founding was the diagnostic abilities of each individual ECG criteria were as follows. ST-segment elevation ≥ 5mm and discordant with the QRS complex: sensitivity 17.1%, specificity 88%, positive and negative post- test probabilities 0.56 and 0.47, respectively. ST segment depression ≥ 1 mm in lead V1, V2 or V3: sensitivity 10.5%, specificity 94%, positive and negative post-test probabilities 0.62 and 0.47, respectively.

ST-segment elevation ≥ 1 mm and concordant with QRS complex: sensitivity 7.9%, specificity 100%.

Kudenchuk et al. (1999) studied utility of the prehospital electrocardiogram in diagnosing acute coronary syndromes: the Myocardial Infarction Triage and Intervention (MITI) project; In order to determine whether the prehospital electrocardiogram (ECG) improves the diagnosis of an acute coronary syndrome. The study consist of 3,027 consecutive patients with symptoms of suspected acute myocardial infarction, 362 of whom were randomized to prehospital versus hospital thrombolysis and 2,665 of whom did not participate in the randomized trial. Their result showed that ST segment and T and Q wave abnormalities suggestive of myocardial ischemia or infarction were more common on both the prehospital and hospital ECGs of patients with as compared with those without acute coronary syndromes ($p \leq 0.00001$). Those with prehospital thrombolysis were more likely to show resolution of ST segment elevation by the time of hospital admission (14% vs. 5% in patients treated in the hospital, $p = 0.004$). In patients not considered for prehospital thrombolysis, both persistent and transient ST segment and T or Q wave abnormalities discriminated those with from those without acute coronary ischemia or infarction? There for ECG abnormalities are an early manifestation of acute coronary syndromes and can be identified by the prehospital ECG.

Nakauchi Y1 et al(2012) studied quantitative myocardial perfusion analysis using multi-row detector CT in acute myocardial infarction; In order to assess the feasibility of quantitative myocardial perfusion imaging (MPI) in acute myocardial infarction (AMI), using multi-row detector CT (MDCT) with a model-based deconvolution method. Their study consist of Fifteen normal subjects with normal coronary arteries

and 26 patients with AMI after reperfusion therapy underwent MPI with MDCT. Perfusion parameters: tissue blood flow (TBF), tissue blood volume (TBV) and mean transit time (MTT) were obtained and compared with clinical parameters, angiography and single-photon emission CT (SPECT) data. Their result was that the TBF and TBV of infarcted myocardium were significantly lower than those of non-infarcted areas (TBF, 51.96±19.42 vs 108.84±13.29 ml/100 g/min, $p<0.01$; TBV, 4.47±2.23 vs 9.79±2.58 ml/100 g, $p<0.01$). The MTT of infarcted areas did not differ from that of non-infarcted areas. The defect areas on TBV colour maps were significantly associated with peak creatine kinase level, QRS score and SPECT defect score. The ratio of TBF or TBV in the epicardial to endocardial side was significantly higher in infarct myocardium with good collateral circulation than in myocardium with poor/no collateral circulation ($p<0.01$ for both). The TBF measurements with CT- and MR-MPI were in good agreement by linear regression analysis ($R=0.55$, $p<0.01$).

Chapter three
Methodology

The general objective of this study was to identify the size of working aspect of the cardiac and it is performance percentage by systems designed for cardiac SPECT.

3-1 Design of the study

This is a cross-sectional study of a descriptive type.

3-2 Population of the study

patients (male and female), with different ages whom were referred to cardiology clinic for myocardial perfusion scintigraphy evaluation of suspected coronary artery disease(CAD).

3-3 Sample size and type of study

The study consist of 51 patients (male and female), with different ages who were referred to cardiology clinic for myocardial perfusion scintigraphy evaluation of suspected coronary artery disease(CAD), they were selected conveniently.

3-4 Place and duration of the study

International medical center (IMC) in SAUDIA ARABIA, JADDAH. Between(Oct2013-May2014).

3-5 Material used to collect the data

The machine consist of two detectors are mounted next to each other (at 90°) on the gantry this allows a full 180° orbit to be acquired while rotating the gantry only through 90°. Collimator Low energy – general purpose or high resolution is used . Images acquired Anterior , Lt. anterior obloquies and Lt Lateral. Record data from multiple position around the body and uses a computer to reconstruct the information in to transverse , sagittale, coronal and obligue slices through the heart .

3-6 Method of data collection

All the study patients under went myocardial perfusion study. Agents used to evaluate myocardial perfusion is TL201 (thallous chloride) TC 99m sestamibi . During stress injection detecting the decrease of blood flow into myocardium directly. Patient must be fasting 4-6 hours prior to scanning. Cessation of all cardiac medication if possible. (particularly beta blockers if possible). TL 201- radiopharmaceuticalBP, heart rate, ECG should be monitoredduring test . Injection should be administered at the peak of stress and exercise continuous for other 1min to permit the tracer deposition in the

tissues.Activity administered is 50-100 MBq (1.5-3) mCi. Intravenously. 74h physical t1/2.135degree LAO view – preset time 8-10 min /view to record sufficient count densityover the myocardium. Data recorded in in digital formal 64X64 matrix or 128X128 (depending on the field of the detector). Delayed imaging after 3-4 h after injection .No eating of carbohydrate food (glucose accelerates the TL 201 clearance from the myocardium) fasting is OK. 10ml of saline flushing to minimize time TL201 contact with the vines of the arm . The time between injection and imaging should not be more than 5min. Redistribution of Tl201 begins after administration by 30 min and usually completes at 4 hours to determine if there has been any redistribution off thallium in the myocardium. In case of Tc99m (HMIBI) is administered I.V. in a dose of 240 MBq following stress exercise test and imaging is started immediately. There is no redistribution of HMIBI.

3-7 Method of data analysis

The acquired image analyzed by Interactive Data Language (IDL) software where the SPECT image converted to grey scale for segmentation purposes. The threshold value used to segment the image will be obtained from the grey image using histogram function to find the lower end of the FWHM around the maximum count after smooth the image by using 3×3 pixel. The threshold value used to generate a binary image where the region of interest (ROI) contains the values 1 and the other regions contains zero. Then the masked image multiplied by the grey scale image to remove the structure outside the ROI. The ROI then normalized by dividing the segmented ROI by the value of the maximum pixel and multiply by 100. The last step is to select pixels that represent the normal heart function by having the pixels that > 70, then the mild where the pixels counts <70 and >50, moderate where the pixel counts >30 and < 50 and sever < 30 or equal zero. All these region given different color i.e. the

normal presented as green, mild blue, moderate yellow and sever red. Figure 3-1 a flow chart shows the sequence of this process. Then collected data analyzed using SPSS and Excel under windows.

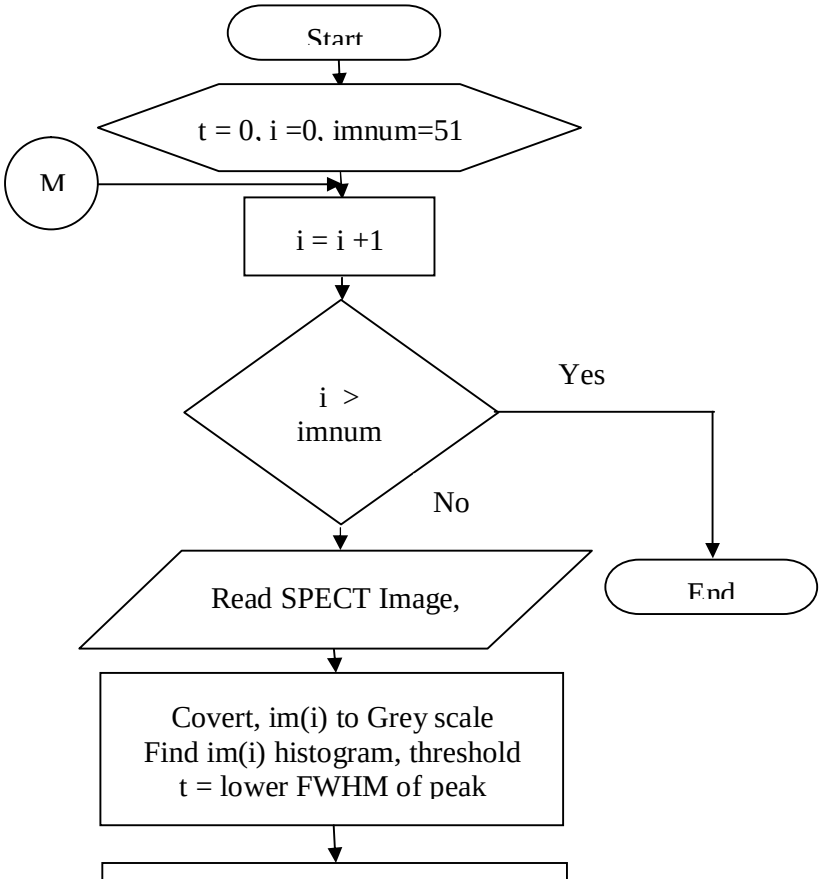

Figure 3-1 a flow chart shows the sequence of image analysis and segmentation using IDL as a platform for calculation.

Chapter four

Results

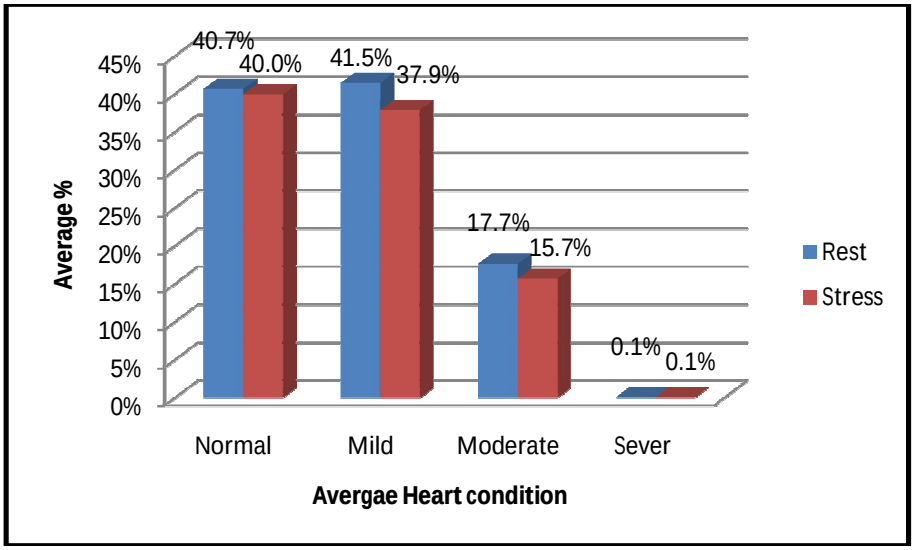

Figure 4-1 a bar graph shows the percentage of the normal, mild, moderate and sever areas of the heart for 51 patients at rest and stress condition.

Table 4-1 a significant paired t-test of the heart segment counts between the rest and stress condition

Paired Samples Test		t	Sig. (2-tailed)
Pair 1	Total rest and totalstress	3.215	.002
Pair 2	Normalrest and Normalstress	1.535	0.131
Pair 3	Mildrest and Mildstress	2.987	0.004
Pair 4	Moderaterest and moderatestress	2.393	0.020
Pair 5	Severrest and Severstress	0.773	.443

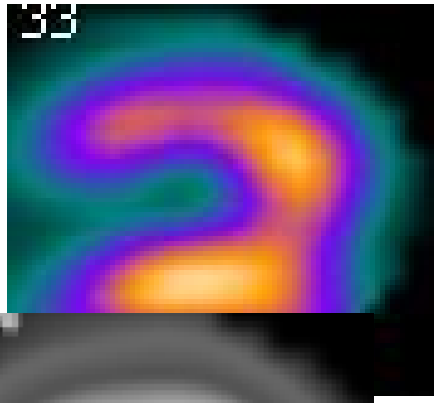

(a)

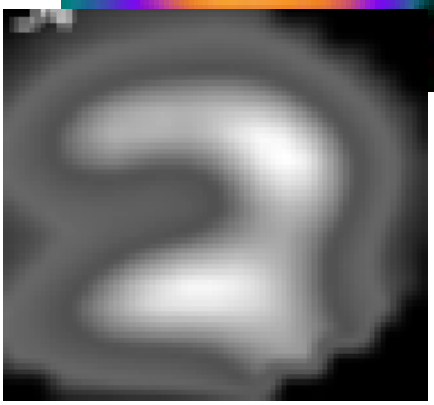

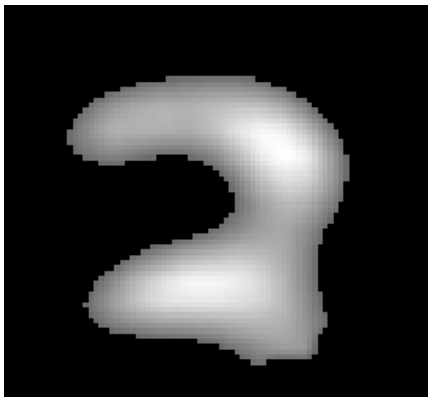

(b)(c)

(D)

(e)

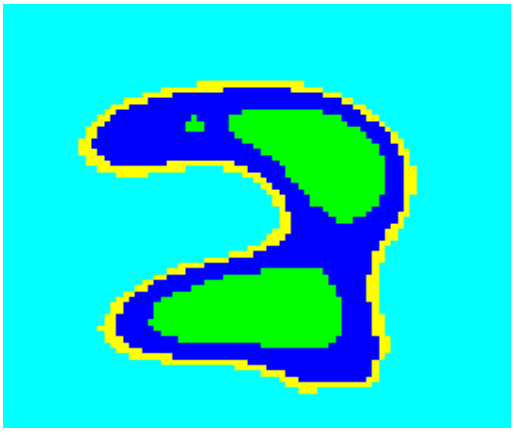

Figure4-2 SPECT heart image of patient at rest (A), while (B) show a grey scale image of the SPECT image, (C) the mask image of the grey scale image, (D) the segmented heart image using the mask image and (E) the classified image according to the maximum pixel counts, where the green, blue, yellow and red color represent normal, mild, moderate and sever count reduction.

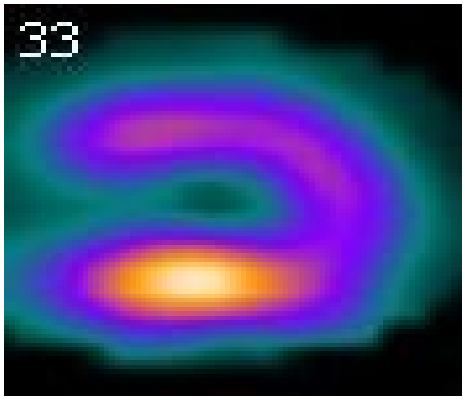

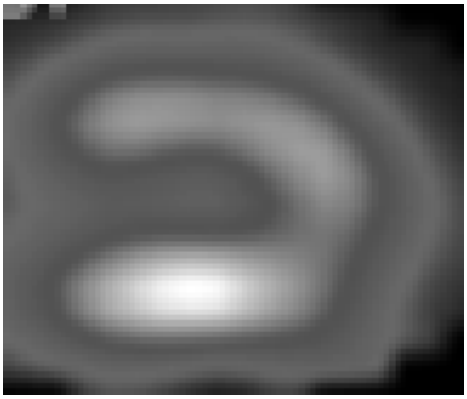

(A) (B)

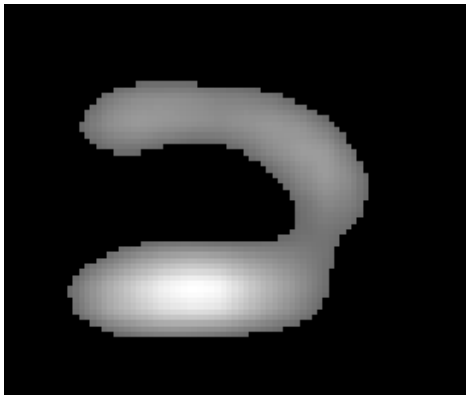

(C) (D)

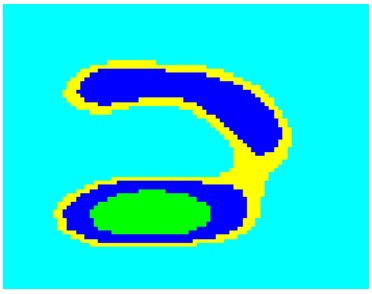

(E)

Figure4-3 SPECT heart image of patient at stress (A), while (B) show a grey scale image of the SPECT image, (C) the mask image of the grey scale image, (D) the the mask image and segmented heart image using according to the (E) the classified image Where the green, blue, maximum pixel counts. represents normal, yellow and red color count reduction. mild, moderate and sever

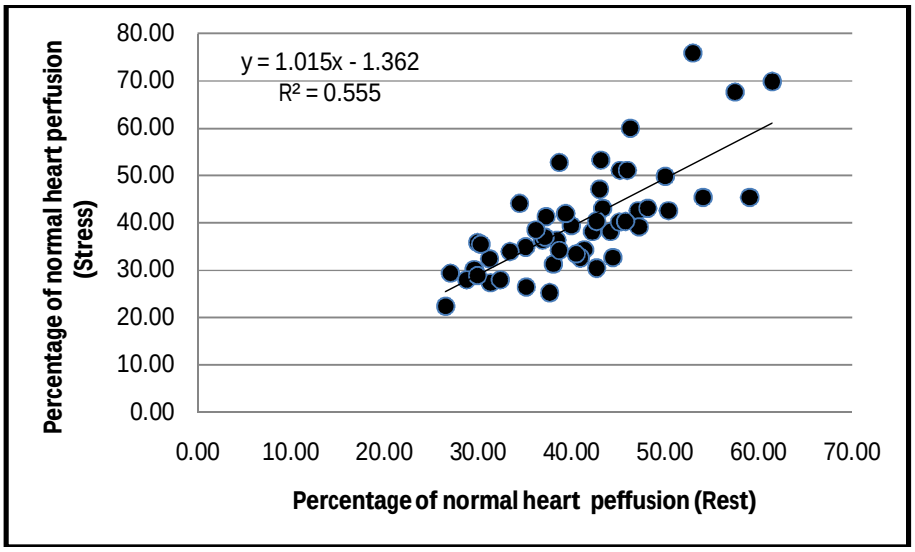

Figure 4-4 scatter plot portrayed a direct linear relationship between the percentage of the normal heart segments at rest and stress.

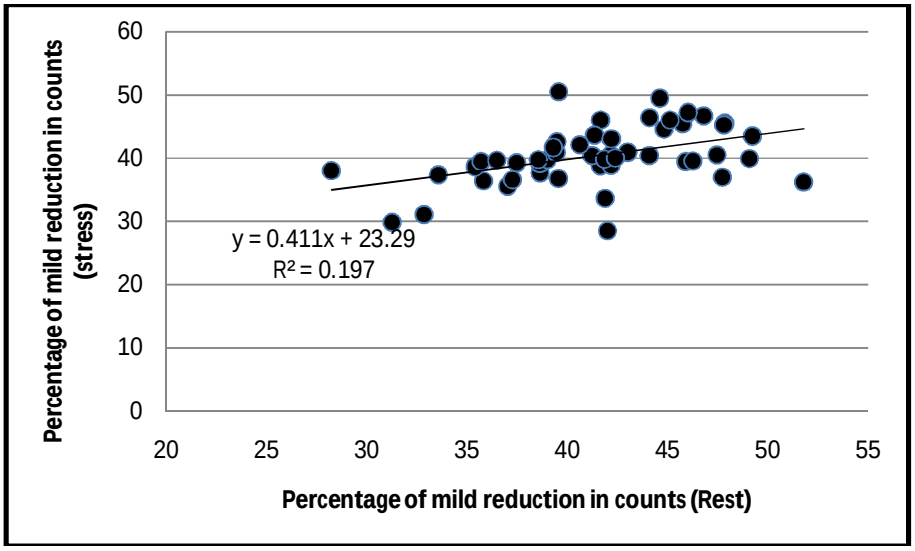

Figure 4-5 scatter plot portrayed a direct linear relationship between the percentage of the mild heart function at rest and stress

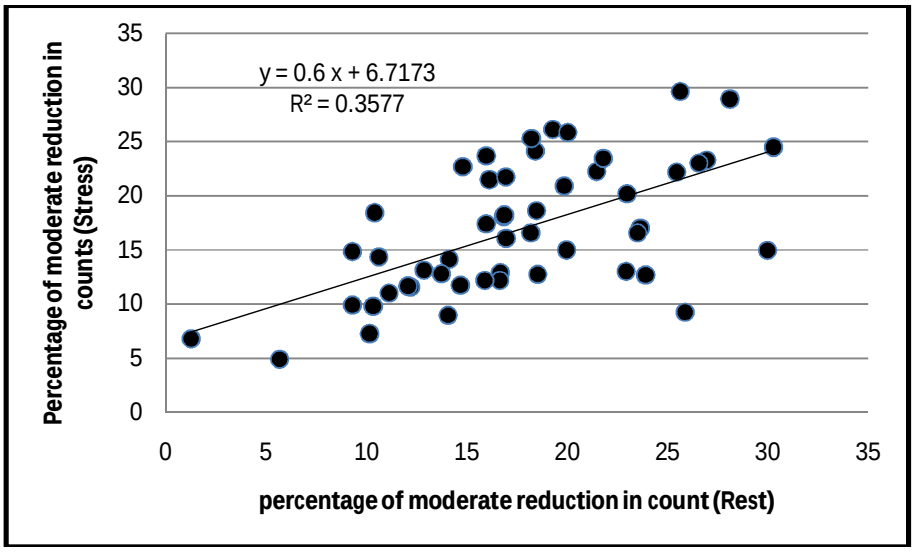

Figure 4-6 scatter plot portrayed a direct linear relationship between the percentage of the moderate heart function at rest and stress

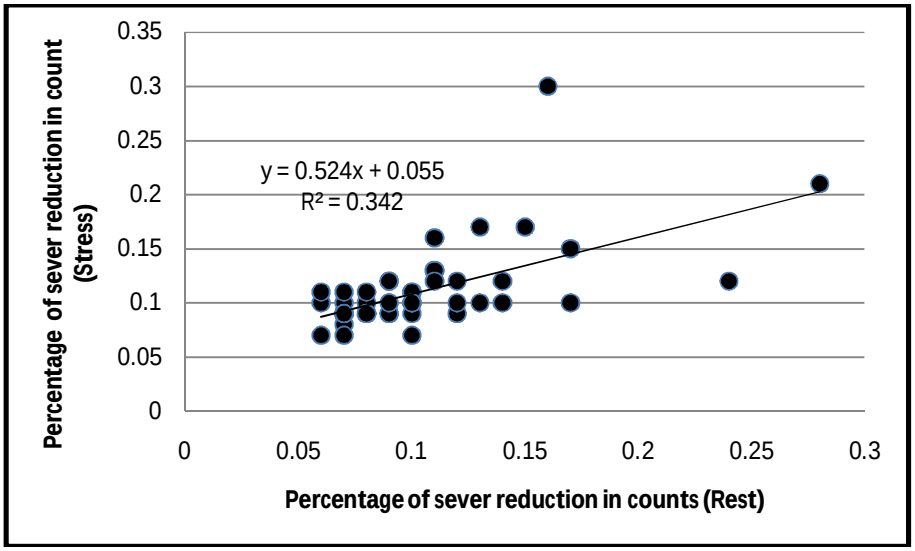

Figure 4-7 scatter plot portrayed a direct linear relationship between the percentage of the sever heart function at rest and stress

Chapter five
Discussion, Conclusion and Recommendation

5-1 Discussion

The data of this study collected from 51 patients underwent heart SPECT examination to identify the percentage of the normal and abnormal percent of the functioning heart size. Out of 51 patient the average size of the normally function heart was 40% during the rest and stress; this represents areas with counts more than 70%, while for the mild area which is represents areas with counts >50% and <70% the results showed that the for the rest condition there is 42% while in the stress condition these areas reduced in average to 37.9%. Similarly for moderate which represents an areas with counts >30% and <50% at rest 17.7% and 15.7 for the stress condition; for sever score in average percentage it was 0.1% for the rest and stress (Figure 4-1).

The results showed that there is a significant difference between the functioning percentage of the heart at rest and stress concerning the mild and moderate classification of heart perfusion reduction at $p = 0.05$ using paired *t*-test, with t equal 1.53 and 2.98 respectively with $p<0.02$. While the normal functioning parts of the heart and the sever condition at rest and stress they don't reveal statistically significant difference with $t = 1.53$ and 0.77 respectively with $p> 0.1$. But the total function of the heart in rest and stress collectively showed a significant difference with $t = 3.21$ and $p = 0.02$ (Table 4-1). This results indicates that the normal function heart areas doesn't affected by rest and stress condition, while for the mild and moderate affected by the stress condition where the counts reduced as shown in Figure 4-3 in contrast to Figure 4-2 which portrayed the rest condition.

The result also showed that there is direct linear association between the normal, mild, moderate and sever heart size percentage at rest and stress. In case of normal heart where there is no significant difference the linear regression equation showed a coefficient equal to 1.01 percent; that means for each one percent of the heart size at rest there is 1.01% as shown in Figure 4-4.

Similarly for the mild, moderate and sever showed a regression coefficient equal to 0.4, 0.6 and 0.5 respectively in stress versus one percent in rest. This result indicate that at stress the count reduced to it is half value of the rest which dictate male function while for the normal hear size areas there is no effects.

5-2 Conclusion

The main objective of this study was to characterize the heart in SPECT images by I identifying the function of the heart areas as normal, mild, moderate and sever according to the perfusion exam at rest and stress condition.

A numbers of the studies were conducted to evaluate the heart function objectively; SPECT examination has a great proportion. All these studies are trial to have a quantitative analysis of the heart performance to overcome the visual perception concept; where subjective outcome will be the evaluation method. Some of these studies focus on developing automatic quantization of regional myocardial wall motion and thickening from gated technetium-99m Sestamibi myocardial perfusion. While others focused on quantitative methods in the evaluation ofThallium-201 myocardial perfusion images; in order to develop quantitative methods to assist the observer in the evaluation of thallium-201 myocardial perfusion images.

The data of this study collected from 51 patients with different age referred to cardiology clinic for myocardial perfusion scintigraphy evaluation of suspected coronary artery disease (CAD). The patient injected with1.5-3 mCi. Intravenously with TL201 (thallous chloride) TC 99m sestamibi. The images were taken at rest and after stress.

The result of this study showed that for normal areas of the heart there is no significant change between the size of this areas in stress and rest condition, while in case of mild, moderate and sever the reduction almost equal to half in stress versus that of the rest; which gives a significant difference between the rest and stress condition at $p = 0.05$.

In summary this study showed that the heart SPECT images can be manipulated using image processing technique, where the region of interest can be segmented using histogram threshold method to create a mask image that can be used to segment the

ROI from the image then the heart image segmented or classified according to their counts as normal, mild, moderate and sever image. Bu summing these portions from each slice we can have the size or percentage of the normal heart function and the affected portions quantitatively.

5-3 Recommendation

- Further studies should be done to include all the view images i.e. Apex to base and inferior anterior.
- Also further studies could be done to locate the area of the defect by reconstructing the heart image in 3D-plane in rest and stress.
- The applied method in this study can be used in the hospital for overall evaluation of the heart function condition instead of the commercial program where interpretation of their illustrated result need a trained personnel by the manufacturer, which is not happened most of the time.

References

Alderman EL, Corley SD, Fisher LD, Chaitman BR, Faxon DP, Foster ED, Killip T, Sosa
JA, Bourassa MG. Five-year angiographic follow-up of factors associated with progression of coronary artery disease in the Coronary Artery Surgery Study (CASS).
CASS Participating Investigators and Staff. J Am Coll Cardiol 1993;22:1141–1154

Alfieri O, La Canna G, Giubbini R, Pardini A, Zogno M, Fucci
C. Recovery of myocardial function. The ultimate target of coronary revascularization.
Eur J Cardiothoracic Surg 1993;7:325–330

Altehoefer C, Kaiser HJ, Deorr R, Feinendegen C, Beilin I, Uebis R, Buell U.
Fluorine-18 deoxyglucose PET for assessment of viable myocardium in perfusion defects in 99mTc-MIBI SPET: a comparative study in patients with coronary artery disease.
Eur J Nucl Med 1992;19:334–342

Altehoefer C, Dahl J vom, Biedermann M, Uebis R, Beilin I, Sheehan F, Hanrath P, Buell U. Significance of defect severity in technetium-99m-MIBI SPECT at rest to assess myocardial viability: comparison with fluorine-18-FDG PET. J Nucl Med 1994;35:569–574

Anagnostopoulos C, Harbinson M, Kelion A, et al. Procedureguidelines for radionuclide myocardial perfusionimaging. Heart 2004; 90 (Suppl):i1–i10.

Metcalfe MJ, NortonMY, Jennings K,Walton S. Improveddetection of abnormal left ventricular wall motion usingtomographic radionuclide ventriculography compared toplanar radionuclide and single plane contrast ventriculography.
Br J Radiol 1993; 66:986–993.

Germano G. Technical aspects ofmyocardial SPECT imaging.
J Nucl Med 2001; 42:1499–1507.
Eisner RL, Nowak DJ, Pettigrew R, et al. Fundamentals
of 180-degree acquisition and reconstruction in SPECTimaging.
J Nucl Med 1986; 27:1717–1728.
O'Connor MK, Kemp B, Anstett F, et al. A multicenterevaluation of commercial
attenuation compensation techniquesin cardiac SPECT using phantom models.
J NuclCardiol 2002; 9:361–376.
Radionuclide angiography. In: Iskandrian AS, PhiladelphiaVMS, eds.
Nuclear Cardiac Imaging: Principles and Application.
Philadelphia: FA Davis; 1996: 144–218.

Appendix A

Master data sheet collection showed number of pixels in the heart for normal, mild, moderate and sever areas at rest and stress condition.

Number	Normal rest	Normal stress	Mild rest	Mild stress	moderate rest	moderate stress	Sever rest	Sever stress
1	3706	3352	3041	2624	1112	986	8	8
2	3776	3299	5025	3370	3253	2028	8	8
3	4878	4216	4603	4304	1555	838	8	8
4	5071	4213	5138	2654	2046	1018	8	8
5	3572	3179	3060	3165	1277	1738	8	8
6	4295	4285	3184	2970	1106	1098	8	8
7	3668	4150	3582	3700	862	1314	8	8
8	2867	3713	2081	2914	1238	1170	8	8
9	4652	4633	5560	4604	3053	2334	8	8
10	4011	3471	6081	3851	2282	2330	8	10
11	3164	3289	4641	3602	2327	1034	8	8
12	3344	2774	2539	2218	1194	1101	8	8
13	4850	3865	4441	3944	2546	2235	8	8
14	3414	3789	3578	3487	2169	1492	8	8
15	3206	3844	4730	4028	2775	804	8	8
16	2374	2422	3387	3203	2259	2292	11	8
17	3449	4941	2688	3649	370	445	8	8
18	2570	3510	3444	2359	618	645	16	8
19	3454	2849	4174	2612	1452	1154	8	8
20	2247	1656	1999	1920	809	1114	8	14

21	4112	4672	1891	3245	680	621	8	8
22	2595	2561	2781	2679	1657	1044	8	8
23	2617	3357	3561	4535	1406	1811	21	20
24	3420	3236	3758	3604	1718	2421	8	8
25	4615	3872	3025	3487	889	1665	8	8
26	3188	3543	2477	3181	1262	1337	8	8
27	6731	5168	4514	6102	145	821	8	8
28	3278	3856	1785	1948	635	721	8	8
29	2910	2463	5244	2733	2817	2189	8	8
30	3346	2994	2875	2804	718	630	8	8
31	3839	3909	4196	3413	3446	1291	8	8
32	2823	2782	3038	2789	1192	1242	8	8
33	3419	3402	3306	2797	1159	826	8	8
34	3319	4101	2970	4655	1404	2969	8	8
35	3403	3007	4177	2609	1210	825	8	8
36	3815	3443	3671	3475	1533	1326	14	14
37	3815	3364	3740	3705	776	1235	8	8
38	4502	3811	2940	2085	1489	820	8	8
39	3578	3921	3715	4991	1017	1168	14	10
40	3882	3871	3899	3437	2663	2085	8	8
41	4662	3852	4560	3348	2288	1903	10	8
42	4955	3325	5553	4622	2636	2776	8	12
43	1646	1792	2822	1901	1621	1107	8	8
44	4027	4298	4301	2082	1899	932	8	8
45	2520	2458	4318	3245	1913	1751	15	11
46	2388	2797	3102	3451	2390	2028	8	8
47	3268	3481	4329	3753	1438	1004	8	8
48	4100	3878	4335	4218	1160	1070	8	8
48	3781	2852	5146	3909	1824	1880	8	8
50	4528	3232	4500	3471	1571	1966	8	8
51	2120	2044	3263	2411	1696	648	8	8

Appendix B

Continuation of master data sheet collection showed % of normal, mild, moderate and sever areas at rest and stress condition.

Normal rest (%)	Normal stress (%)	Mild rest (%)	Mild stress (%)	moderate rest (%)	moderate stress (%)	Sever rest (%)	Sever stress (%)
47.11	48.09	38.66	37.65	14.13	14.15	0.1	0.11
31.3	37.9	41.66	38.71	26.97	23.3	0.07	0.09
44.17	45.01	41.68	45.95	14.08	8.95	0.07	0.09
41.35	53.38	41.9	33.62	16.68	12.9	0.07	0.1

45.12	39.3	38.65	39.12	16.13	21.48	0.1	0.1
49.98	51.25	37.05	35.52	12.87	13.13	0.09	0.1
45.17	45.25	44.11	40.34	10.62	14.33	0.1	0.09
46.29	47.57	33.6	37.34	19.99	14.99	0.13	0.1
35.05	40.01	41.89	39.76	23	20.16	0.06	0.07
32.39	35.92	49.11	39.86	18.43	24.12	0.06	0.1
31.2	41.46	45.77	45.41	22.95	13.03	0.08	0.1
47.2	45.47	35.84	36.35	16.85	18.05	0.11	0.13
40.95	38.45	37.49	39.24	21.49	22.23	0.07	0.08
37.23	43.17	39.02	39.73	23.66	17	0.09	0.09
29.91	44.27	44.13	46.38	25.89	9.26	0.07	0.09
29.56	30.56	42.17	40.42	28.13	28.92	0.14	0.1
52.94	54.64	41.26	40.35	5.68	4.92	0.12	0.09
38.66	53.82	51.81	36.17	9.3	9.89	0.24	0.12
38.01	43.02	45.93	39.44	15.98	17.42	0.09	0.12
44.38	35.2	39.48	40.82	15.98	23.68	0.16	0.3
61.46	54.67	28.26	37.97	10.16	7.27	0.12	0.09
36.86	40.7	39.5	42.58	23.53	16.59	0.11	0.13
34.41	34.53	46.82	46.64	18.49	18.63	0.28	0.21
38.41	34.91	42.21	38.88	19.29	26.12	0.09	0.09
54.06	42.87	35.43	38.61	10.41	18.43	0.09	0.09
45.97	43.91	35.72	39.42	18.2	16.57	0.12	0.1
59.05	42.71	39.6	50.43	1.27	6.79	0.07	0.07
57.45	59.02	31.28	29.82	11.13	11.04	0.14	0.12
26.51	33.32	47.76	36.97	25.66	29.61	0.07	0.11
48.16	46.52	41.38	43.57	10.34	9.79	0.12	0.12
33.41	45.34	36.52	39.59	29.99	14.98	0.07	0.09
39.98	40.79	43.03	40.89	16.88	18.21	0.11	0.12
43.32	48.37	41.89	39.77	14.69	11.74	0.1	0.11
43.1	34.95	38.57	39.67	18.23	25.3	0.1	0.07
38.68	46.63	47.48	40.46	13.75	12.79	0.09	0.12
42.23	41.69	40.64	42.08	16.97	16.06	0.15	0.17
45.75	40.47	44.85	44.57	9.31	14.86	0.1	0.1
50.36	56.68	32.89	31.01	16.66	12.2	0.09	0.12
42.98	38.86	44.63	49.46	12.22	11.58	0.17	0.1
37.14	41.18	37.3	36.56	25.48	22.18	0.08	0.09
40.47	42.28	39.58	36.75	19.86	20.89	0.09	0.09
37.67	30.97	42.22	43.06	20.04	25.86	0.06	0.11
27	37.27	46.29	39.54	26.59	23.02	0.13	0.17
39.35	58.72	42.02	28.44	18.55	12.73	0.08	0.11
28.75	32.93	49.26	43.47	21.82	23.46	0.17	0.15
30.27	33.76	39.33	41.66	30.3	24.48	0.1	0.1
36.14	42.21	47.87	45.51	15.9	12.18	0.09	0.1
42.69	42.27	45.14	45.98	12.08	11.66	0.08	0.09
35.14	32.97	47.83	45.2	16.95	21.74	0.07	0.09

42.69	37.25	42.42	40	14.81	22.66	0.08	0.09
29.91	39.99	46.04	47.17	23.93	12.68	0.11	0.16

Appendix C

SPECT images used to Quantize the heat function

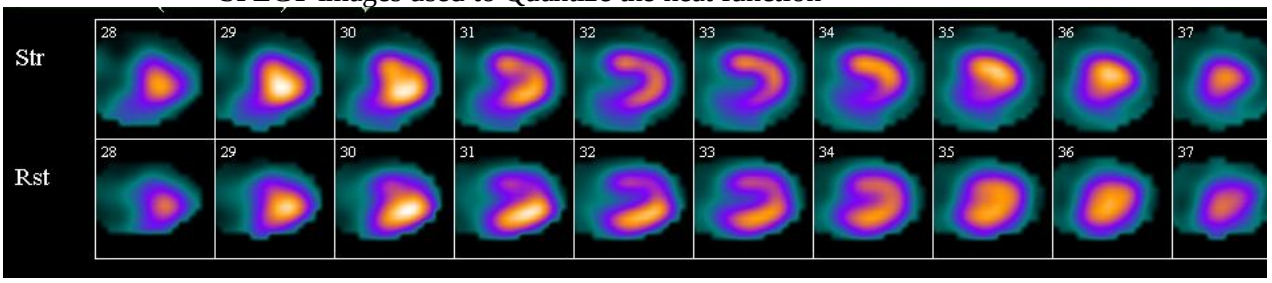

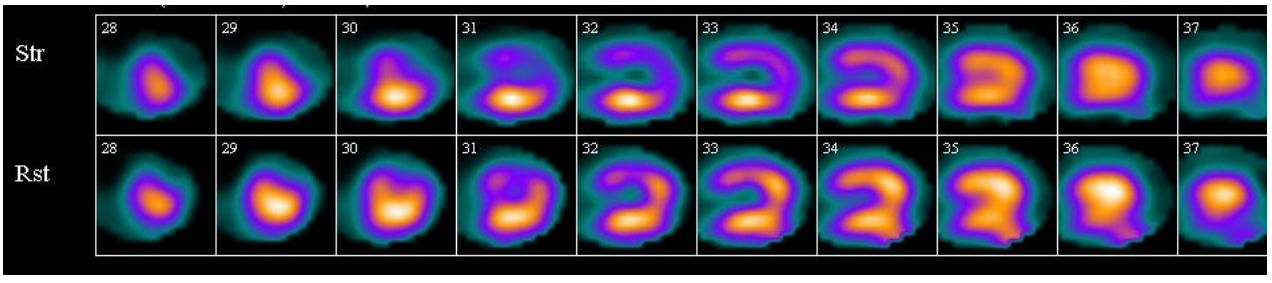

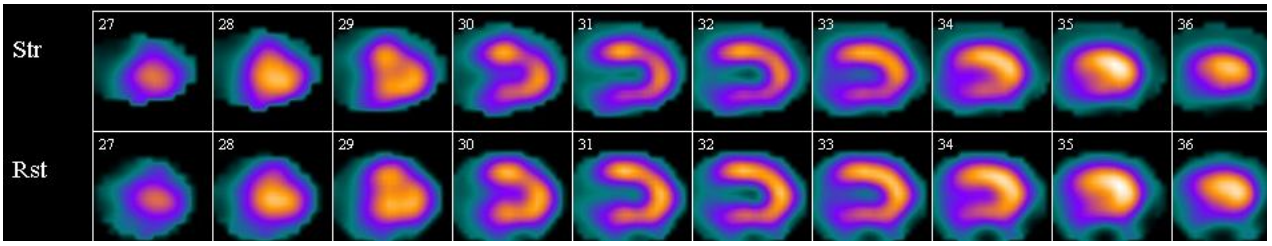
Str
27 28 29 30 31 32 33 34 35 36
Rst
27 28 29 30 31 32 33 34 35 36

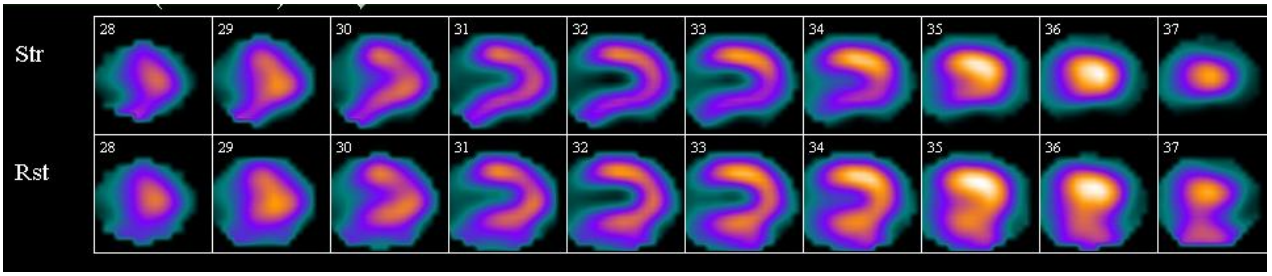
Str
28 29 30 31 32 33 34 35 36 37
Rst
28 29 30 31 32 33 34 35 36 37

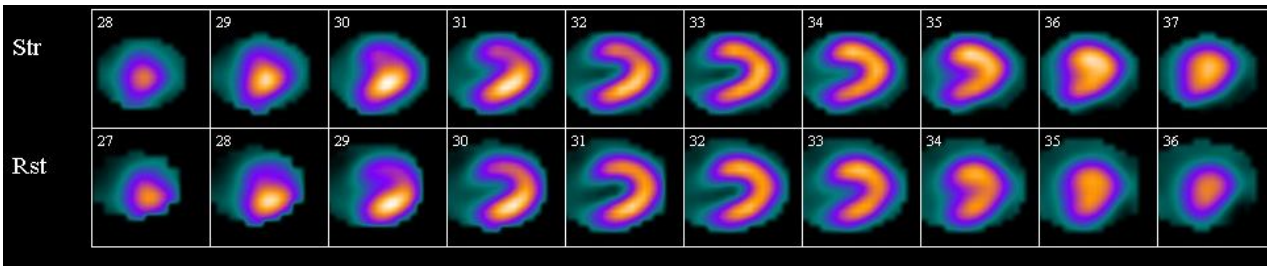
Str
28 29 30 31 32 33 34 35 36 37
Rst
27 28 29 30 31 32 33 34 35 36

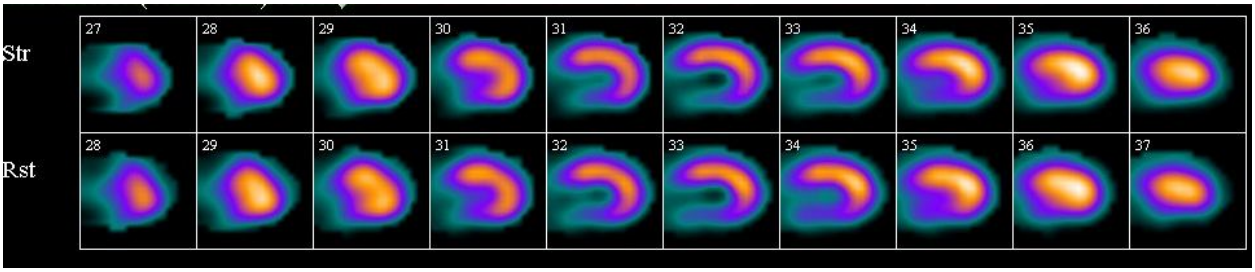
Str
27 28 29 30 31 32 33 34 35 36
Rst
28 29 30 31 32 33 34 35 36 37

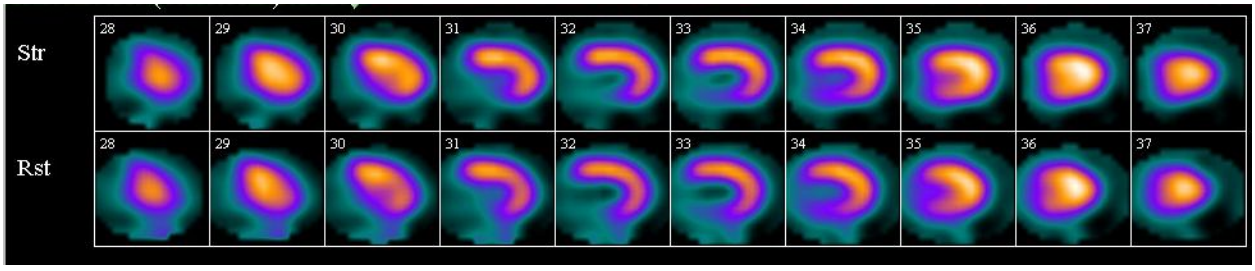
Str
28 29 30 31 32 33 34 35 36 37
Rst
28 29 30 31 32 33 34 35 36 37

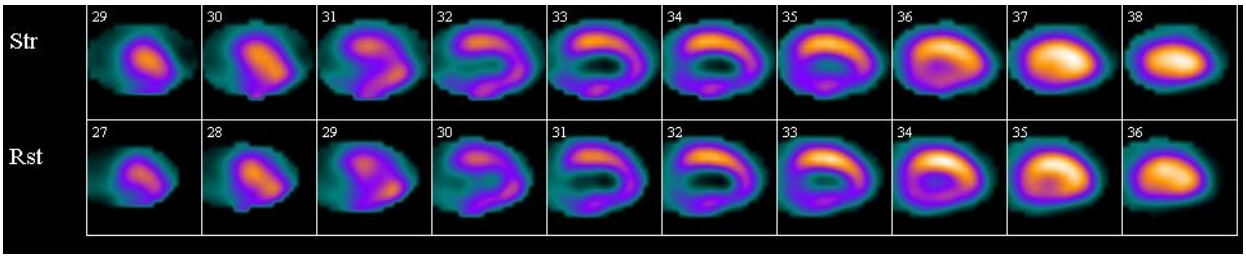
Str
29 30 31 32 33 34 35 36 37 38
Rst
27 28 29 30 31 32 33 34 35 36

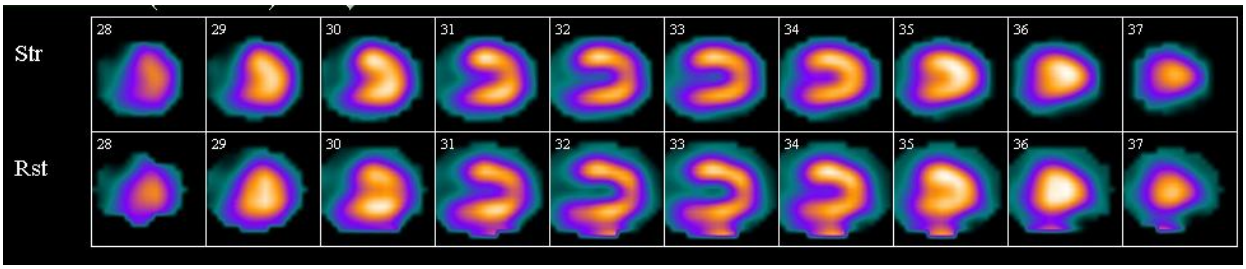
Str
28 29 30 31 32 33 34 35 36 37
Rst
28 29 30 31 32 33 34 35 36 37

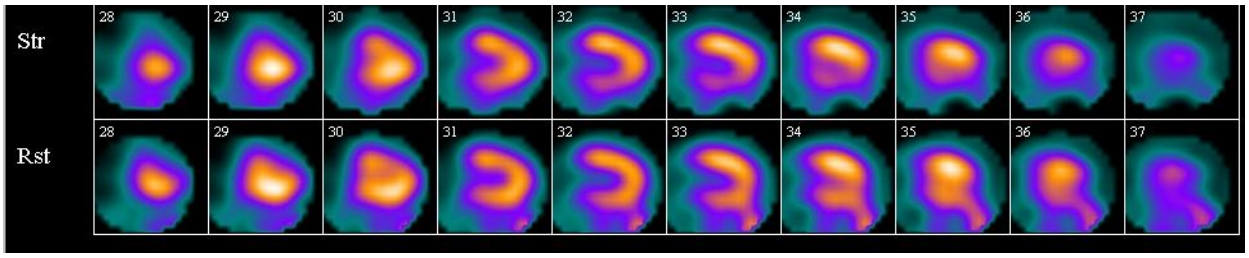
Str
28 29 30 31 32 33 34 35 36 37
Rst
28 29 30 31 32 33 34 35 36 37

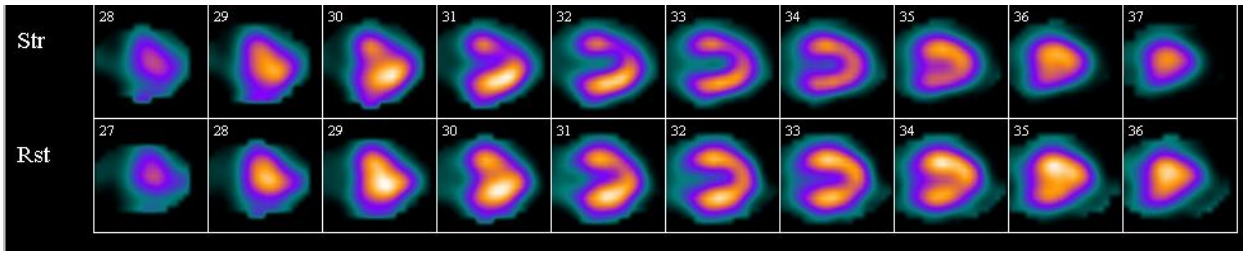
Str
28 29 30 31 32 33 34 35 36 37
Rst
27 28 29 30 31 32 33 34 35 36

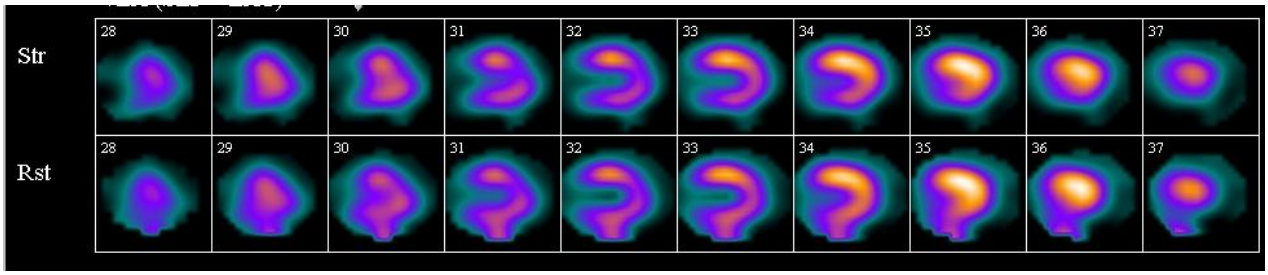
Str
28 29 30 31 32 33 34 35 36 37
Rst
28 29 30 31 32 33 34 35 36 37

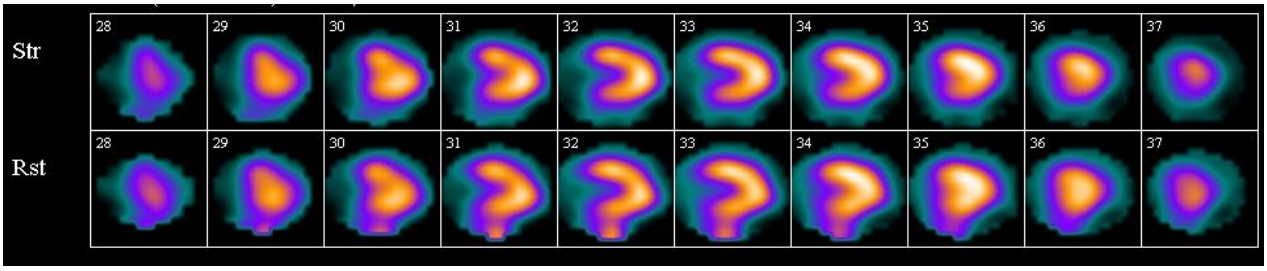
Str
28 29 30 31 32 33 34 35 36 37
Rst
28 29 30 31 32 33 34 35 36 37

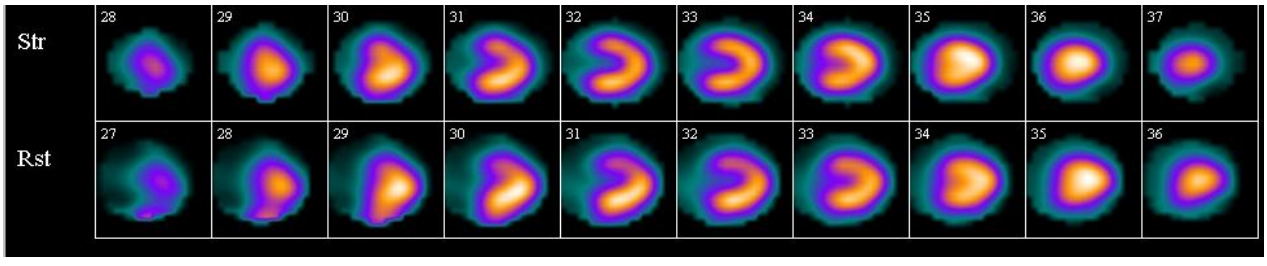
Str
28 29 30 31 32 33 34 35 36 37
Rst
27 28 29 30 31 32 33 34 35 36

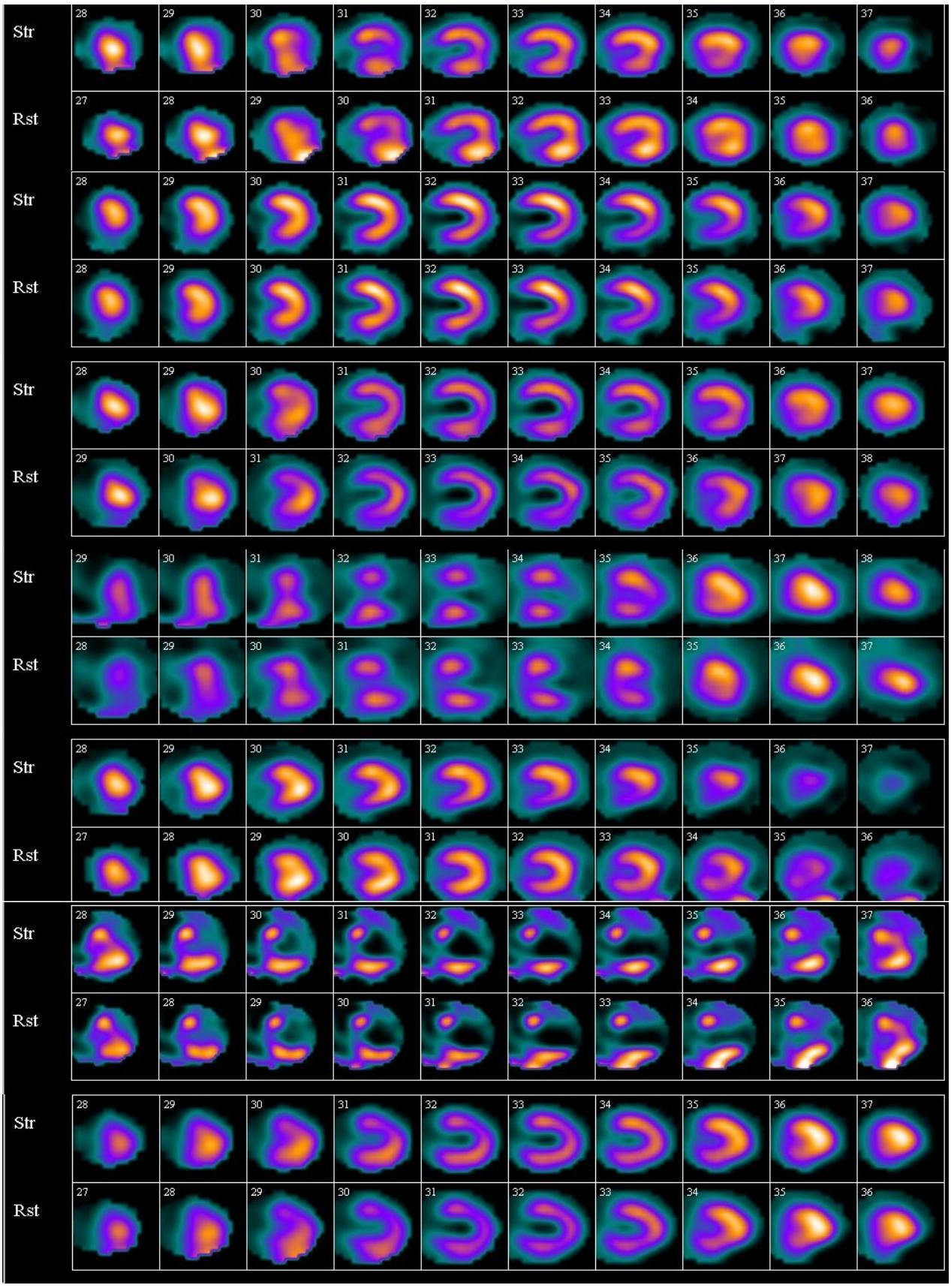
Str
Rst
Str
Rst
Str
Rst
Str
Rst
Str
Rst
Str
Rst

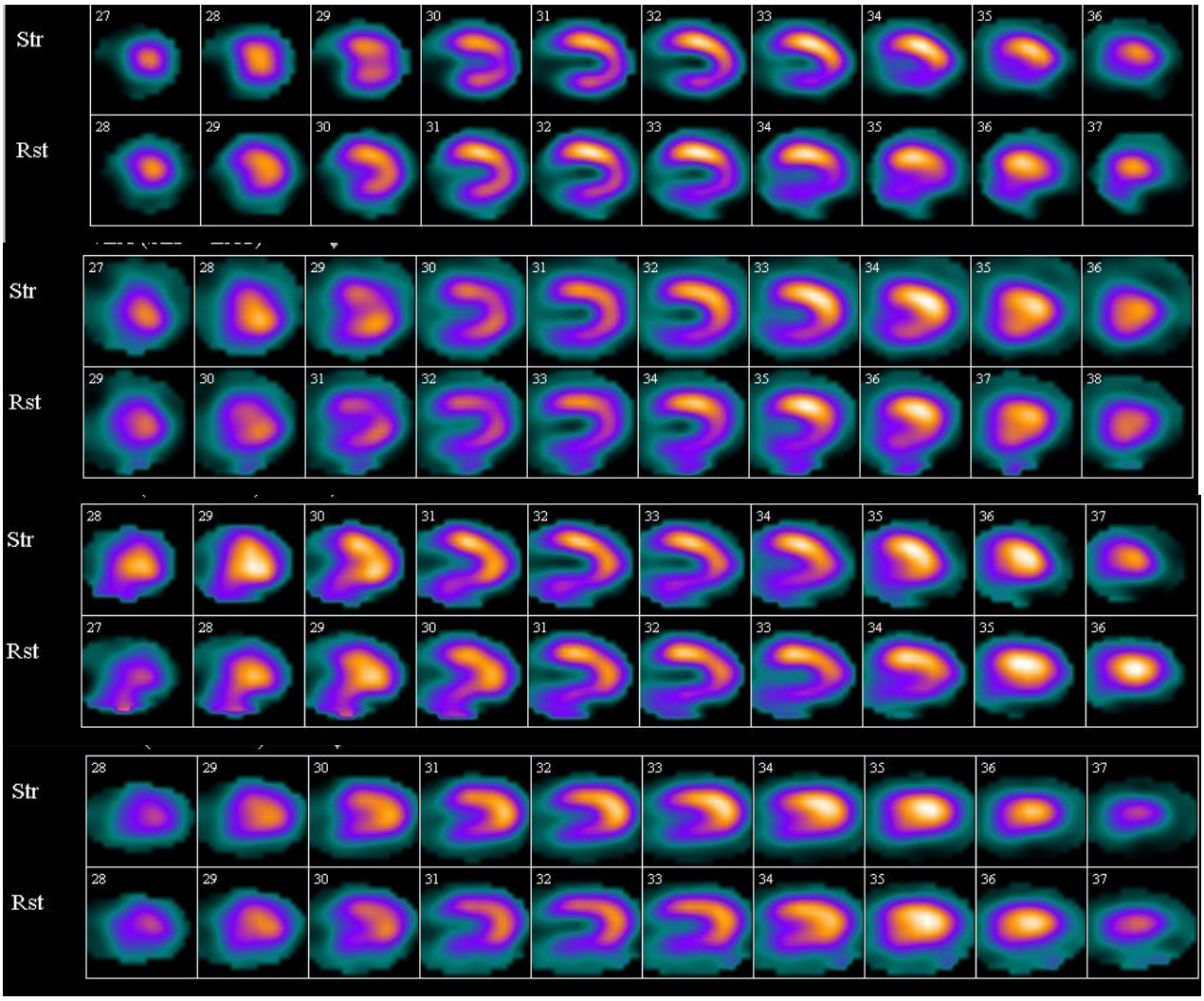
Str
27 28 29 30 31 32 33 34 35 36
Rst
28 29 30 31 32 33 34 35 36 37
Str
27 28 29 30 31 32 33 34 35 36
Rst
29 30 31 32 33 34 35 36 37 38
Str
28 29 30 31 32 33 34 35 36 37
Rst
27 28 29 30 31 32 33 34 35 36
Str
28 29 30 31 32 33 34 35 36 37
Rst
28 29 30 31 32 33 34 35 36 37